



Short communication

Properties and fuel cell performance of a Nafion-based, sulfated zirconia-added, composite membrane

M.A. Navarra, C. Abbati, B. Scrosati*

Dipartimento di Chimica, Università di Roma "La Sapienza", 00185 Rome, Italy

ARTICLE INFO

Article history:

Received 18 March 2008

Received in revised form 14 April 2008

Accepted 14 April 2008

Available online 22 April 2008

Keywords:

Proton membranes

Sulfated zirconia

Composite membrane

Fuel cells

ABSTRACT

The effect of an acidic inorganic additive, i.e. sulfated zirconia, on Nafion-based polymer electrolytes is evaluated by comparing the properties in terms of conductivity and fuel cell performance of a composite sulfated zirconia-added Nafion membrane with those of an additive-free Nafion membrane. The peculiar surface properties of the selected filler promote a higher hydration level and a higher conductivity for the composite membrane under unsaturated conditions, i.e. at 20% RH. Tests on H₂-air fully humidified cells, monitored at 70 °C and at atmospheric pressure, reveal small differences when passing from a plain Nafion to a composite Nafion/sulfated zirconia membrane as electrolyte. However, remarkably great improvements are observed for the composite membrane-based cell when the comparison tests are run at low relative humidity and high temperature, this outlining the beneficial role of the sulfated zirconia additive.

© 2008 Elsevier B.V. All rights reserved.

1. Introduction

A wide spread commercialization of polymer electrolyte membrane fuel cells, PEMFCs, is presently set back by the limitations imposed by the currently available polymer membranes [1]. The state-of-art membranes, i.e., perfluorinated sulfonic membranes, such as Nafion™, due to the strong dependence on water content of its proton conductivity [2], limit the operation temperature of PEMFCs to 80 °C under strict humidification requirements.

In the research of high temperature proton-exchange membranes with adequate performances at low relative humidity, an attractive strategy consists of the incorporation of inorganic acidic compounds within the Nafion-type matrix [3–7]. The addition of an inorganic solid acid into conventional polymeric electrolytes has the dual function of improving water retention and of providing additional acidic sites. According to the cluster network model for ionomers, the Nafion microstructure can be visualized as formed by hydrophobic domains (i.e., the fluorinated backbone) and hydrophilic domains, the latter consisting of ionic clusters comprising the sulfonic acid moiety and the absorbed water [8,9]. These clusters are interconnected by a network of short and narrow channels and the size of the clusters is strongly dependent on the system water content [10]. Considering the mechanisms of proton transport [11], one may assume that the presence of the

inorganic additive, when uniformly dispersed at low particle size in the Nafion matrix, may favourably affect the ionic conductivity, indeed, the hydration water of the additive can form bridges between shrunken clusters [7] and, in virtue of its acidity, the filler can provide additional pathways for proton hopping from one cluster to another.

In this respect, sulfated zirconium oxide (herein after "SZr") is recently attracting interest as fuel cell membrane additive thanks to its extraordinary high acidity [12–14]. Deeply studied as catalyst for the conversion of organic compounds [15–17], SZr has been rarely investigated as proton conductor. Hara et al. found that surface SO₄ species existed as bidentate complexes strongly bonded with ZrO₂ in a SZr powder calcined at 620 °C. SO₄ species are electron-withdrawing and, thus, the Lewis acidity of zirconium is strengthened. The Lewis points can easily convert to Brønsted acid points in the presence of water, these finally acting as proton donors [18].

The use of a superacidic inorganic compound has been already considered in our laboratory by evaluating the effect of a commercial SZr micrometric additive on the properties of Nafion-based composite membranes [19]. The conductivity of the SZr/Nafion membrane was found to be much higher above 100 °C than that associated with plain, additive-free Nafion membranes, as well as with composite Nafion membranes using a standard ZrO₂ additive. In this work we extend the study by investigating the effect of a low-sized in-house-sulfated zirconia when used as additive for new types of Nafion-based composite membranes. We have tested these composite membranes as electrolytes in PEMFCs under different relative humidity and temperature conditions.

* Corresponding author.

E-mail address: bruno.scrosati@uniroma1.it (B. Scrosati).

Table 1
Composition and thickness of the membranes prepared in this work

Membrane name	Nafion (wt.%)	SZr (wt.%)	Thickness (μm)
Nafion	100	–	86
Nafion/SZr	95	5	100

2. Experimental

Sulfated zirconia, SZr, was prepared by treating at room temperature ZrO_2 (Aldrich, sub-micron powder) in an aqueous 0.5 M H_2SO_4 solution under magnetic stirring for 30 min. The suspension was allowed to separate and the liquid removed. The wet powder collected was dried at 150°C and finally calcined for 2 h at 600°C , i.e. at a temperature suitable to produce sulfate groups strongly bonded to the surface of the zirconium oxide [18]. The resulted sulfated powder was stored in an inert atmosphere and grinded before use.

The morphology and the dimension of the particles were evaluated by scanning electron microscopy, SEM, using a LEO 1450 VP apparatus. The sulfated content was estimated by thermal gravimetric analysis, TGA, performed with a TGA/SDTA 851 Mettler-Toledo instrument at a heating rate of $10^\circ\text{C min}^{-1}$ in air flux.

The insertion of inorganic insoluble particles inside a polymer matrix can be achieved by a variety of procedures [20]. In this work, Nafion membranes, both with and without the SZr inorganic additive, were prepared following the recast procedure described in our previous work [19]. Accordingly, the common solvents of a Nafion solution, i.e. 5 wt.% in water and alcohols (Ion Power Inc.) were gradually replaced by *N,N*-dimethylacetamide, DMAc. When required, SZr powder was added and homogeneously dispersed. The mixture was poured on a Petri dish and the solvent evaporated. The resulting dry membranes were hot-pressed at 175°C and 20 atm to improve their thermo-mechanical stability and finally activated and purified by subsequent immersions in boiling hydrogen peroxide (3 vol.%), sulfuric acid (0.5 M) and water. All the membrane samples were stored in distilled water. Table 1 summarizes the composition and the thickness of the membranes prepared in this work.

The thermal properties of the membranes were examined by differential scanning calorimetry, DSC, using a DSC 821 Mettler-Toledo instrument at a scan rate of $20^\circ\text{C min}^{-1}$ in a nitrogen flux.

Ex situ conductivity measurements were performed by using a screwed porous metal cell where the given membrane sample was sandwiched between two commercial electrodes (E-Tek, $0.5 \text{ mg Pt cm}^{-2}$). This conductivity cell was put in a humidity-controlled chamber equipped with temperature and relative humidity control using the Vaisala HMT 330 probe. The membrane sample was dried over night at 70°C before assembling the cell. The measurements were carried out by setting the temperature of the chamber at a given value (i.e., 70°C) and progressively increasing the relative humidity through the inlet of a saturated hot vapor stream. The cell was allowed to stabilize at each experimental conditions for a couple of hours before taking the measurement. The conductivity of the given membrane was evaluated from impedance spectra recorded with a Solartron frequency response analyzer 1255B by applying a 10 mV signal in the 100,000–1 Hz frequency range.

Fuel cell tests were performed by using a compact system (850C, Scribner Associates Inc.) connected to a 5 cm^2 cell fixture. The active surface of the used electrodes (E-Tek, $0.5 \text{ mg Pt cm}^{-2}$) was brushed with a Nafion solution (ca. $0.4 \text{ mg dry Nafion cm}^{-2}$). The membrane-electrode assembly, MEA, was realized by hot pressing the given membrane between two electrodes at 120°C and 2 atm for 7 min. The cell was fed with H_2 and air at atmospheric pressure according to current-dependent mass flow rates. Accordingly,

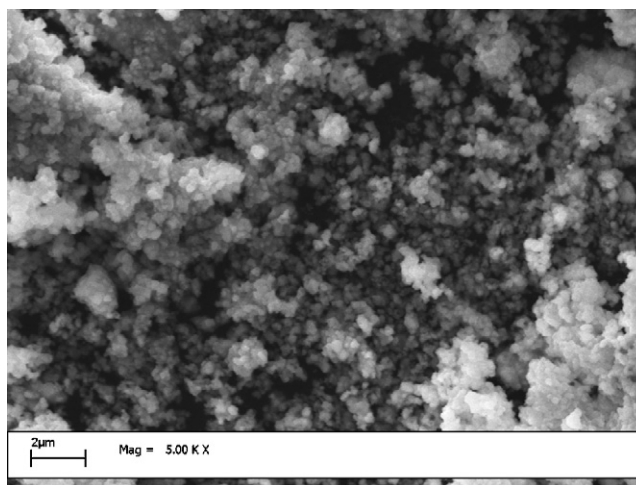


Fig. 1. SEM image of the sulfated zirconia, SZr, prepared in this work.

1.4 times anode stoichiometric flow and 3.3 times cathode stoichiometric flow were programmed. The humidification of the cell was accomplished by bubbling the fed gases through stainless steel cylinders incorporated in the compact system and containing distilled water. Heating tape, wrapped around the feed lines, avoided condensation. The temperature of the humidifiers, as well as that of the cell, was properly set to achieve the desired relative humidity. To be noticed that the relative humidity values were calculated on the basis of water vapor pressure at cell temperature and at humidifiers temperature [21]. Before recording polarization curves as a function of relative humidity, the cell was conditioned by fast current scans, for 2 days at increasing temperature (from 30 to 99°C) under full humidification. The compact fuel cell test system is equipped with an integrated frequency response analyzer (880 Impedance Analyzer) able to add an AC sine wave to the DC current flowing in the cell, in the 10,000–1 Hz frequency range. The amplitude of the sine wave was chosen to be 10% of the DC current present at 0.5 V cell voltage. In situ impedance spectra were obtained with the integrated frequency response analyzer under the same experimental conditions (i.e., cell temperature, relative humidity and gas pressure parameters) used for recording polarization curves.

3. Results and discussion

Fig. 1 shows the SEM image of the sulfated zirconia, SZr, prepared in this work. An homogeneous distribution of sub-micrometric particles, scaling on few hundred nanometers, is evident. By comparing this image to the micrograph (not shown here) of the starting ZrO_2 powder, no particle size or morphology changes could be observed. This suggests that the sulfation process did not produce aggregations.

The sulfation degree of the SZr powder was evaluated by means of thermo-gravimetric analysis, TGA. Fig. 2 reports the TGA responses of a SZr powder before and after being treated in water at 80°C under magnetic stirring. This treatment was carried out in order to assess the hydrothermal stability of the acidic inorganic compound. The weight loss occurring in the region 550 – 750°C is assumed to be due to the decomposition of the SO_4^{2-} groups bound to the ZrO_2 surface and released as sulfur oxides [13]. The SO_4^{2-} content in the sulfated zirconia was estimated from the extent of the weight loss to be about 13 wt.%, with a non-significant reduction after the water treatment (i.e., 10 wt.%, see the dashed-line thermogram in Fig. 2). The weight loss in the lower-temperature range,

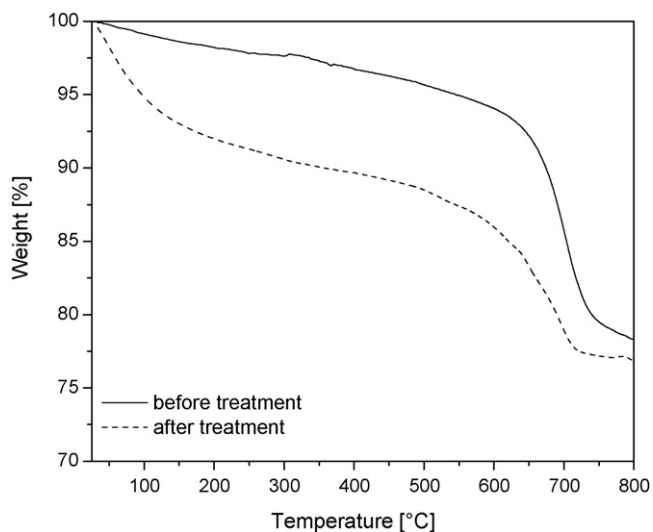


Fig. 2. TGA response of the sulfated zirconia powder before (solid line) and after (dashed line) being treated in water at 80 °C.

starting from 25 °C, can be attributed to the removal of adsorbed water.

The sulfated zirconia, SZr, was dispersed as inorganic additive in a Nafion matrix to prepare the composite membranes, here identified as Nafion/SZr. The thermal properties of these membranes were investigated by differential scanning calorimetry, DSC. Also additive-free membranes were tested for comparison purpose. Fig. 3 shows the result. The DSC response of both membranes consists of a broad endothermic peak. This thermal transition is routinely observed for Nafion-type membranes and it has been attributed to structural changes into polymer ionic clusters with strict connection to the hydration degree of the membrane [22]. Since the absorption of water increases the free volume, thus facilitating the chain mobility, the temperature of occurrence of this peak depends on the water content of the membrane. In addition, as suggested by Gierke et al. [23], an increase in the water absorbed by a membrane increases the number of sulfonic groups per aggregate and, thus, the size of the aggregate; the energy required to overcome the ionic interaction within the highly organized clusters also increases. Table 2 reports the temperature and energy (ΔH) associated with this ionic cluster transition for both the membranes.

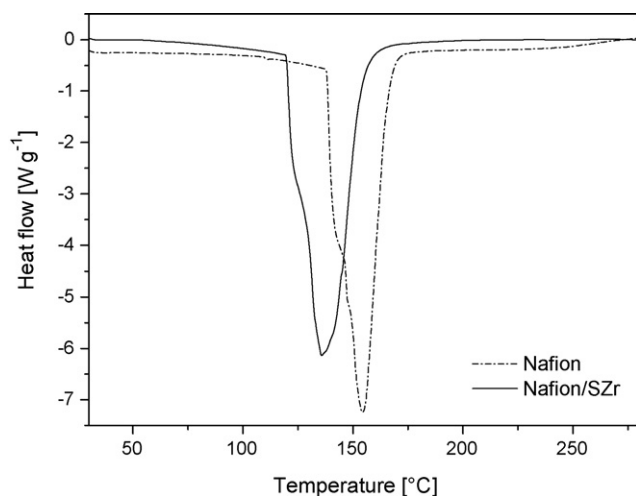


Fig. 3. DSC response of additive-free Nafion and Nafion/SZr composite membranes.

Table 2

Temperature and energy associated to the ionic cluster transition in both additive-free Nafion and composite Nafion/SZr membranes

Membrane	Temperature (°C)	ΔH (J g ⁻¹ polymer)
Nafion	153	343
Nafion/SZrO	135	404

The composite membrane shows lower temperature and higher enthalpy change, thus revealing larger water content with respect to the plain Nafion membrane. This difference is obviously associated with the presence of the inorganic compound and is expected to indirectly affect the transport properties of the composite membrane.

To control this, ex situ conductivity measurements were performed on both the membranes as function of relative humidity, RH. Fig. 4 reports the conductivity detected at 70 °C under three RH values of interest, chosen to simulate working conditions spanning from the dry to the wet state. As expected, the conductivity of both membranes increases with the relative humidity; however, the values of the composite Nafion/SZr membrane are higher over all the examined RH range. Interestingly, the difference peaks at 20% RH, where the conductivity of the composite membrane almost doubles that of the additive-free membrane. This confirms that the inorganic additive, in virtue of both its acidity and hydrophilicity, promotes proton transport even in a not-fully humidified membrane.

In order to investigate whether the beneficial effect of the additive may reflect in the fuel cell performances, two cells were assembled by using either additive-free Nafion or composite Nafion/SZr as electrolyte. For comparison purpose, both cells underwent the same conditioning cycles and their responses were recorded under identical operating parameters. Fig. 5 reports voltage–current and power–current curves obtained by increasing the temperature of anode and cathode humidifiers at a given cell temperature (i.e., 70 °C). This allows MEAs to experience different levels of relative humidity. Both cells improve their performances by increasing the humidifiers temperature, i.e. the relative humidity; however, the cell using the composite Nafion/SZr always delivers the highest power and current values.

The different performances between Nafion- and Nafion/SZr-based cells can be highlighted by evaluating the maximum power and current delivered by each cell in the three working conditions explored, as arising from Fig. 5a–c. The relative variations, Δx , of

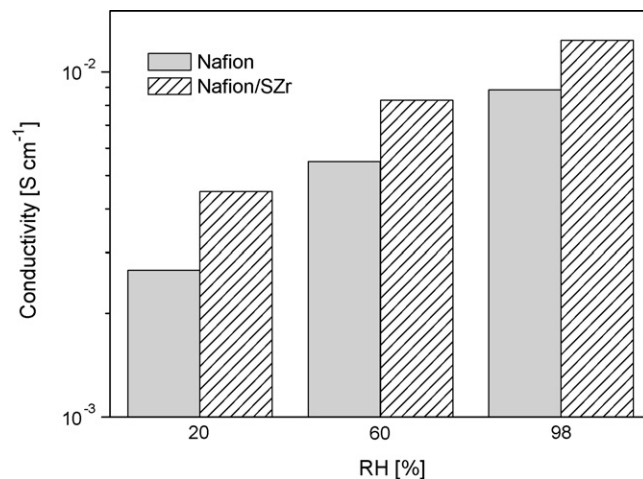


Fig. 4. Conductivity of additive-free Nafion and composite Nafion/SZr membranes at 70 °C as a function of relative humidity, RH.

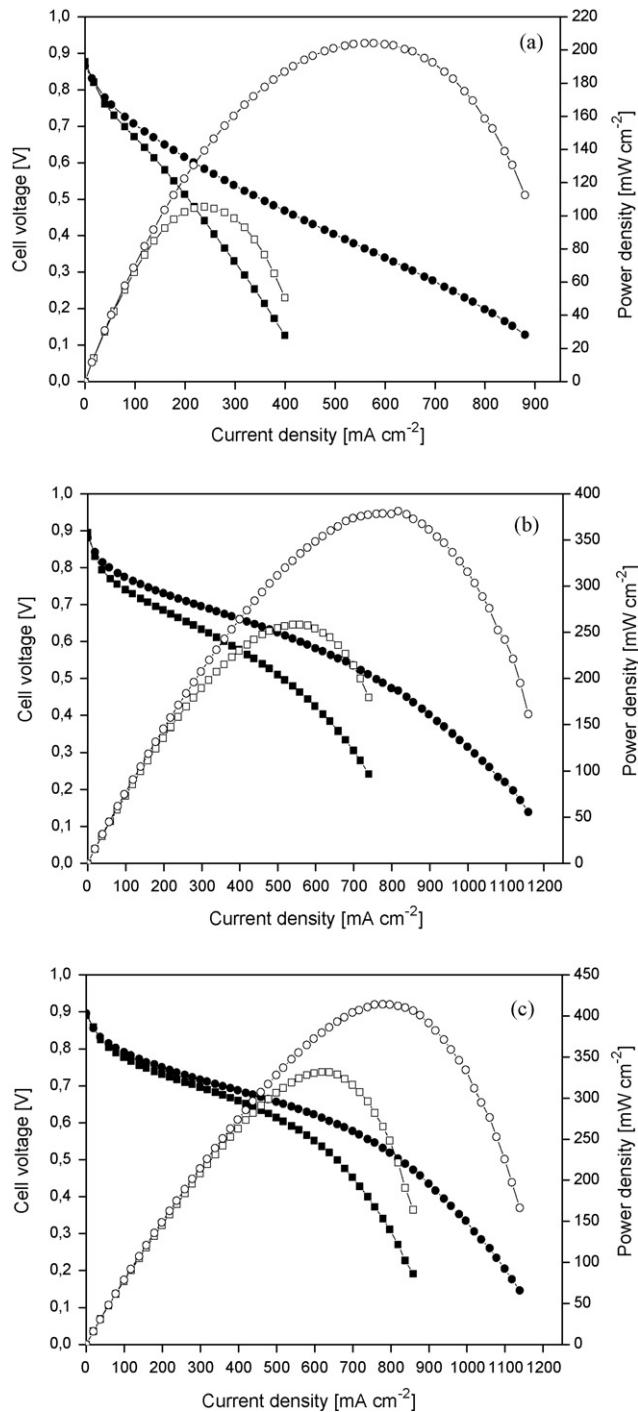


Fig. 5. Fuel cell performances when using additive-free Nafion (■: voltage–current; □: power–current) or composite Nafion/SZr (●: voltage–current; ○: power–current) membrane as electrolyte. $T_{\text{cell}} = 70\text{ }^{\circ}\text{C}$, $P(\text{H}_2\text{-air}) = 1\text{ atm}$. (a) $T_{\text{humidifiers}} = 45\text{ }^{\circ}\text{C}$. (b) $T_{\text{humidifiers}} = 56\text{ }^{\circ}\text{C}$. (c) $T_{\text{humidifiers}} = 70\text{ }^{\circ}\text{C}$.

current and power (Δi and Δp , respectively) between the composite Nafion/SZr-based and the additive-free Nafion-based cell were calculated by the equation:

$$\Delta x\% = \frac{x(\text{Nafion/SZr}) - x(\text{Nafion})}{x(\text{Nafion})} \times 100 \quad (1)$$

where “ x ” is the current density and the power density, corresponding to the maximum of the power–current curves reported in Fig. 5a–c.

Table 3

Relative variations of current, Δi , and power, Δp , corresponding to the maximum of the power–current curves in Fig. 5, for composite Nafion/SZr-based and additive-free Nafion-based cells

$T_{\text{humidifiers}}\text{ (}^{\circ}\text{C)}$	$\Delta i\text{ (}\%\text{)}$	$\Delta p\text{ (}\%\text{)}$
45	135	93
56	46	47
70	26	25

$T_{\text{cell}} = 70\text{ }^{\circ}\text{C}$.

Table 3 lists the results obtained for the two cells differing by the electrolyte membrane. Clearly, the use of the composite Nafion/SZr membrane leads to a greater gain in terms of maximum power/current. Remarkably, this gain in performance, expressed by the relative variations reported in Table 3, is high when the relative humidity is low (i.e., $T_{\text{cell}} = 70\text{ }^{\circ}\text{C}$ and $T_{\text{humidifiers}} = 45\text{ }^{\circ}\text{C}$) and becomes progressively less important with the increase of the humidifiers temperature.

In order to further investigate this aspect, an impedance analysis was carried out on cells based either on additive-free Nafion or on composite Nafion/SZr membrane as electrolyte. The cells were kept at 0.5 V and at $70\text{ }^{\circ}\text{C}$, under low (i.e., $T_{\text{humidifiers}} = 45\text{ }^{\circ}\text{C}$) and high (i.e., $T_{\text{humidifiers}} = T_{\text{cell}} = 70\text{ }^{\circ}\text{C}$) relative humidity. Fig. 6 shows the relative Nyquist plots.

It is reasonable to assume that the high frequency intercept on the real axis is representative of the cell resistance while that at the low frequency is representative of the charge transfer resistance. Fig. 6 shows that no significant differences between the two cells can be detected for the high frequency intercept at a given RH value; this reveals that the bulk resistance does not play a key role in determining the different fuel cell response of the two MEAs at a given relative humidity. However, the width of the semi-circles is considerably higher in the case of the cell based on additive-free Nafion under low relative humidity (see Fig. 6a), this revealing that the charge transfer resistance greatly changes when passing from one cell to the other. This in turn demonstrates that the use of conventional, plain Nafion-based cell may result in cells having a poor membrane–electrode interface contact under low RH

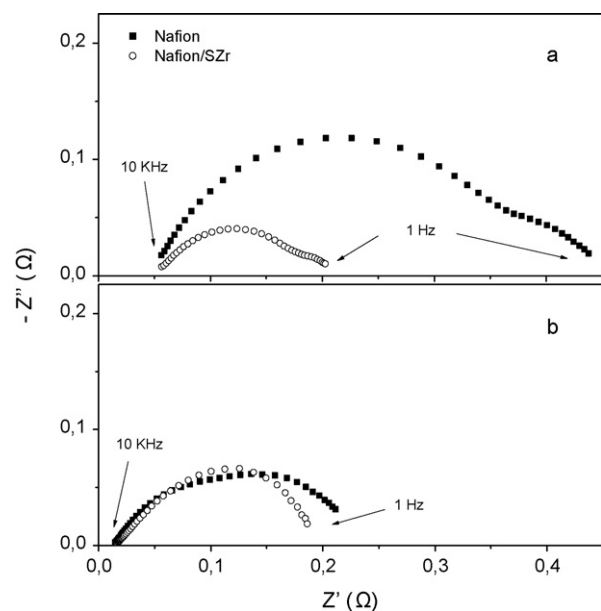


Fig. 6. Impedance spectra of additive-free Nafion-based (■) and composite Nafion/SZr-based (○) fuel cells recorded at 0.5 V. $T_{\text{cell}} = 70\text{ }^{\circ}\text{C}$. (a) $T_{\text{humidifiers}} = 45\text{ }^{\circ}\text{C}$; (b) $T_{\text{humidifiers}} = 70\text{ }^{\circ}\text{C}$.

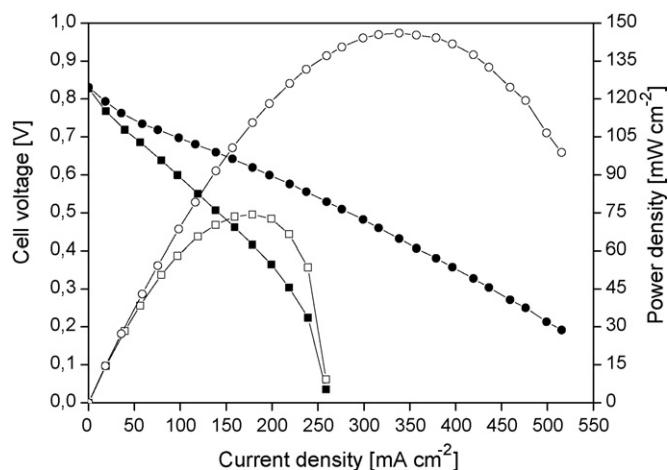


Fig. 7. Fuel cell performances when using additive-free Nafion (■: voltage–current; □: power–current) or composite Nafion/SZr (●: voltage–current; ○: power–current) membrane as electrolyte. $T_{\text{cell}} = 110^{\circ}\text{C}$, $T_{\text{humidifiers}} = 91^{\circ}\text{C}$, $P(\text{H}_2\text{-air}) = 1\text{ atm}$.

conditions ($T_{\text{cell}} = 70^{\circ}\text{C}$ and $T_{\text{humidifiers}} = 45^{\circ}\text{C}$ correspond to 30% RH ca.), probably because of ionomer shrinkage [12,24]. This important result highlights the role of the inorganic filler in enhancing low-RH fuel cell performance in virtue of its unique role in stabilizing membrane–electrode interface. Surely, at low RH and high temperatures, the shrinkage and dehydration of the ionomer present in the catalyst layer also need to be addressed.

Finally, the effect of temperature has been investigated by examining the performance of the two cells at 110°C with the humidifiers temperature set at 95°C , corresponding to an intermediate relative humidity of ca. 50%. Fig. 7 shows voltage–current and power–current curves obtained under the mentioned conditions. The response of both cells is undoubtedly reduced with respect to that obtained at 70°C under comparable humidity level (i.e., $T_{\text{humidifiers}} = 56^{\circ}\text{C}$); however, the cell using the composite membrane as electrolyte still shows the best performance with a gain, in terms of relative variation of maximum power, as high as 97%.

4. Conclusion

The beneficial role of a sulfated zirconia in promoting the performance of Nafion-based membranes has been demonstrated by

both ex situ and in situ analyses. The high water affinity and the intrinsic acidity of the inorganic additive enhance the conductivity of the composite membrane and allow the cells using it to operate at low relative humidity levels. In addition, the use of SZr-based composite membranes also improves the high temperature response. Work is in progress in our laboratory to further optimize the interfacial resistance by incorporating the additive in both membrane and catalyst layers in order to increase the homogeneity of the cell structure. Finally, a time-stability test is currently under development to assess long-term fuel cell performances.

Acknowledgements

This work has been performed in the framework of the NUME Project, titled “Development of composite proton membranes and of innovative electrode configurations for polymer electrolyte membrane fuel cells” supported by the Italian Ministry of University and Research, MIUR, program FISR 2001.

References

- [1] J. Larminie, A. Dicks, Fuel Cell Systems Explained, 2nd ed., Wiley, 2003.
- [2] Y. Sone, P. Ekdunge, D. Simonsson, J. Electrochem. Soc. 143 (1996) 1254–1259.
- [3] S. Malhotra, R. Datta, J. Electrochem. Soc. 144 (1997) L23.
- [4] B. Tazi, O. Savadogo, Electrochim. Acta 45 (2000) 4329.
- [5] C. Yang, P. Costamagna, S. Srinivasan, J. Benziger, A.B. Bocarsly, J. Power Sources 103 (2001) 1.
- [6] A.S. Aricò, V. Baglio, A. Di Blasi, V. Antonucci, Electrochem. Commun. 5 (2003) 862.
- [7] V. Ramani, H.R. Kunz, J.M. Fenton, J. Membr. Sci. 232 (2004) 31.
- [8] T.D. Gierke, J. Electrochem. Soc. 124 (1977) 319c.
- [9] K.D. Kreuer, J. Membr. Sci. 185 (2001) 29.
- [10] W.Y. Hsu, T.D. Gierke, Macromolecules 15 (1982) 101.
- [11] K.D. Kreuer, Chem. Mater. 8 (1996) 610.
- [12] T.M. Thampan, N.H. Jalani, P. Choi, R. Datta, J. Electrochem. Soc. 152 (2005) A316.
- [13] Y. Zhai, H. Zhang, J. Hu, B. Yi, J. Membr. Sci. 280 (2006) 148.
- [14] S. Ren, G. Sun, C. Li, S. Song, Q. Xin, X. Yang, J. Power Sources 157 (2006) 724.
- [15] C.L. Bianchi, S. Ardizzone, G. Cappelletti, Surf. Interface Anal. 36 (2004) 745.
- [16] D.J. Zaleski, S. Alerasool, P.K. Doolin, Catal. Today 53 (1999) 419.
- [17] M.K. Mishra, B. Tyagi, R.V. Jasra, J. Mol. Catal. A: Chem. 223 (2004) 61.
- [18] S. Hara, M. Miyayama, Solid State Ionics 168 (2004) 111.
- [19] M.A. Navarra, F. Croce, B. Scrosati, J. Mater. Chem. 17 (2007) 3210.
- [20] G. Alberti, M. Casciola, Annu. Rev. Mater. Res. 33 (2003) 129.
- [21] K.T. Adjemian, R. Dominey, L. Krishnan, H. Ota, P. Majsztrik, T. Zhang, J. Mann, B. Kirby, L. Gatto, M. Velo-Simpson, J. Leahy, S. Srinivasan, J.B. Benziger, A.B. Bocarsly, Chem. Mater. 18 (2006) 2238.
- [22] S.H. de Almeida, Y. Kawano, J. Therm. Anal. Calorim. 58 (1999) 569.
- [23] T.D. Gierke, E. Munn, F.C. Wilson, J. Polym. Sci., Polym. Phys. Ed. 19 (1981) 1687.
- [24] K. Kanamura, H. Morikawa, T. Umegaki, J. Electrochem. Soc. 150 (2003) A193.